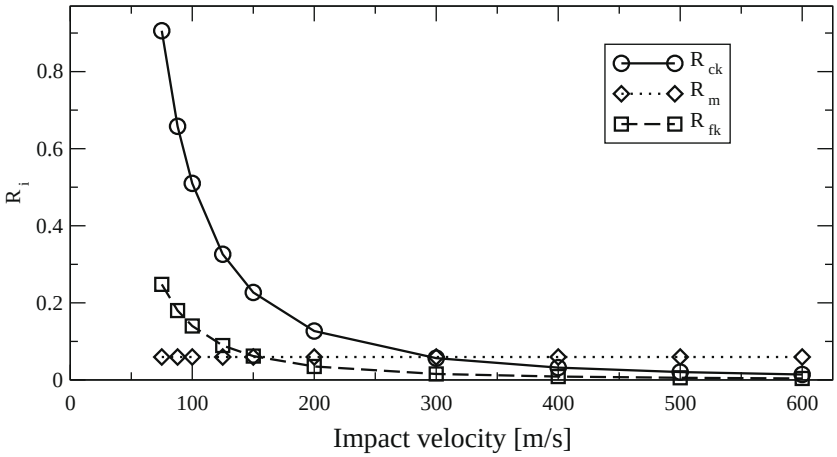

Fig. 8. R_{ck}, R_{fk} and R_m as function of impact velocity.

Fig. 9. Gas gun experimental device.

captured. A sequence recorded by the high speed camera is shown in Fig. 10.

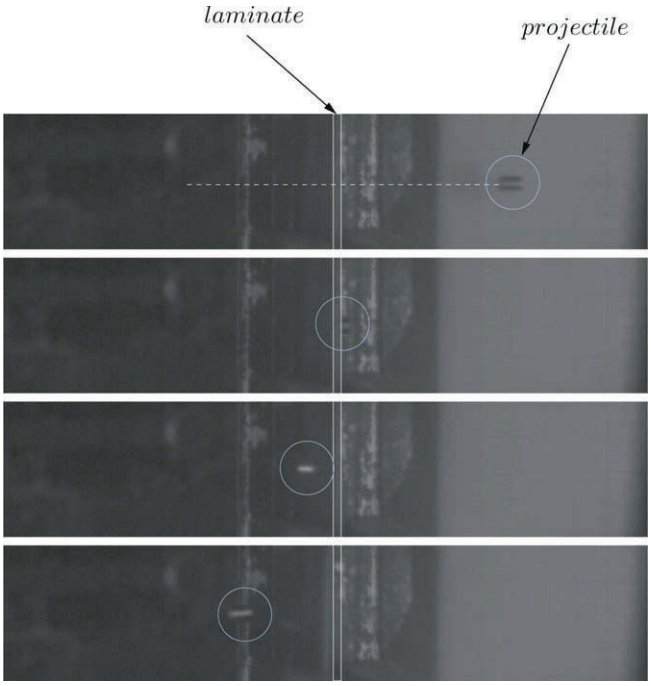

Fig. 10. Sequence of an impact process.

6. Results

6.1. Validation

To validate the proposed model, impacts at velocities between 100 and 400 m/s were performed. This wide range of velocities al lows to perform the validation above and below the ballistic limit. Fig. 11 shows the residual velocity of the projectile for different im pact velocities; experimental and analytical results are compared. The model predicts with high accuracy the residual velocity and in addition estimates the minimum impact velocity of the projec tile needed to perforate the laminate, which is around 130 m/s for this combination of laminate and projectile. As the impact velocity increases, the curve tends to a straight line, which is the expected result.

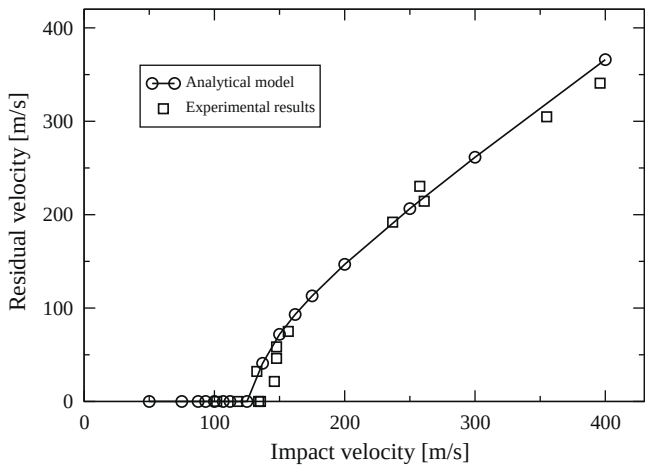

Fig. 11. Residual velocity vs. impact velocity; analytical and experimental results.

6.2. Analysis of the energy absorption mechanisms

Fig. 12 shows the relative importance of each absorption mech anism as a function of the impact velocity. As the impact velocity increases, the term related to the linear momentum transfer increases its relative importance, reaching the 60% of the total en

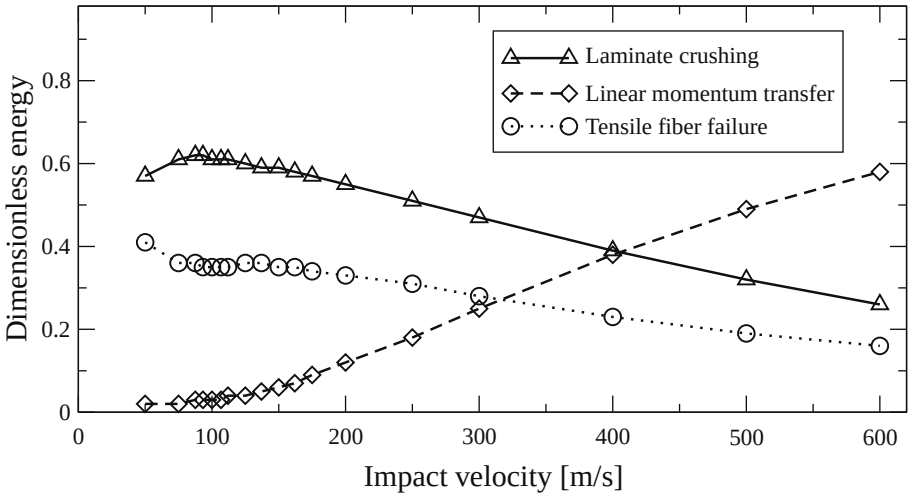

Fig. 12. Dimensionless energy vs. impact velocity.

ergy absorbed by the laminate when the projectile impact velocity is 600 m/s. The trend of the other two energy absorption mecha nisms (tensile fiber failure and laminate crushing) is almost the same for velocities above the ballistic limit (around 130 m/s): its importance decreases as the impact velocity increases because both mechanisms do not vary significantively with impact velocity. However, below ballistic limit its trends are different. Laminate crushing increases with impact velocity because more thickness of the laminate is involved in the penetration process. Tensile fiber failure decreases, because it starts to play a role only after $t \quad t_0$; then, at low velocities this mechanism initiates when the projectile is closer to the impact face and involves more plies of the laminate.

6.3. Influence of the projectile size

In this section, an analysis of the influence of the projectile as pect ratio in the ballistic behavior of the laminate is presented. Fig. 13 shows the residual velocity vs. impact velocity for different projectile masses, keeping the radius constant. This variation rep resents a change in the density or in the length of the projectile. As m_p increases the ballistic limit decreases and the curve tends to an asymptote which is the graph bisector. When the projectile mass tends to infinity, keeping the thickness and the density of the laminate constant, the ratio R_m tends to zero and the residual velocity equals the impact velocity. In Fig. 13, the last curve corre sponds to $m_p \quad 50$ g, which is three orders of magnitude greater than the laminate mass affected by the impact ($\rho_l Ah$).

Fig. 14 shows the evolution of the ballistic limit, as a function of the projectile mass keeping constant its radius. The curve has two

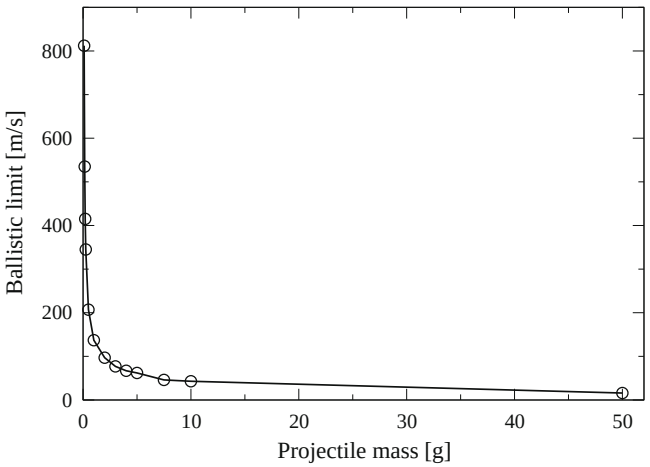

Fig. 14. Ballistic limit vs. projectile mass; constant radius.

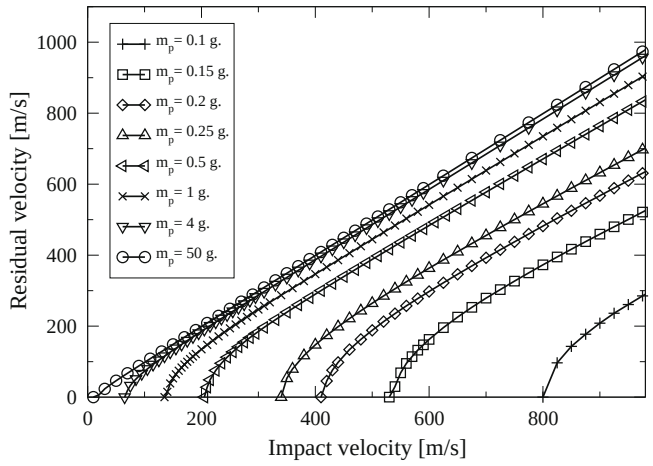

Fig. 13. Residual velocity vs. impact velocity, for different projectile masses; constant radius.

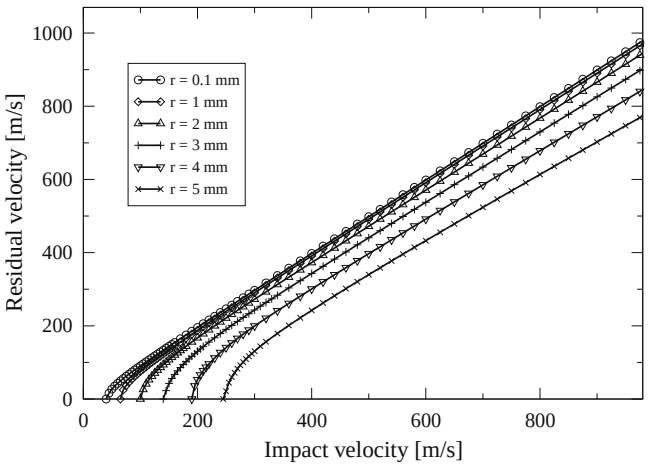

Fig. 15. Residual velocity vs. impact velocity, for different projectile radius; constant mass.

asymptotes: the abscissa and the ordinate. When the projectile mass tends to infinity the ballistic limit tends to zero, and when the mass tends to zero, the impact velocity needed to penetrate the laminate tends to infinity. This graph shows the prediction capability of the developed model, and demonstrates that it pro vides expected tendencies in a wide range of projectile masses.

Finally Fig. 15 presents the residual velocity vs. impact velocity for different projectile radii keeping the mass constant; this varia tions means (as for Fig. 13) that the density of the projectile or its length is modified. As the radius decreases the curve tends to an asymptote which is the graph bisector (residual velocity equal to impact velocity), since the laminate zone affected by the impact is proportional to the frontal projectile area. As the radius increases the curve moves to the right, the ballistic limit also increases, and the slope corresponding to the high velocity regime decreases.

7. Conclusions

An analytical model to predict the residual velocity of cylindri cal projectiles after impacting thin carbon/epoxy woven laminates has been developed. The model considers three different energy absorption mechanisms for the laminate. As a summary of this work, the following conclusions could be found:

- The analytical model developed, predicts with accuracy the residual velocity of steel cylinder projectiles when penetrating carbon/epoxy woven laminates.
- The use of quasi static test (punch and crushing) to obtain a reli able value of the through thickness compressive strength of the laminate as a function of the depth of penetration is appropriate to estimate the energy absorbed by the composite by laminate crushing.
- Using the analytical model developed in this work as a pre design tool, it is possible to obtain trustworthy results of the influences of different problem parameters, such as projectile geometry or material.

Acknowledgment

This research was done with the financial support of the University Carlos III of Madrid and of the Comunidad Autónoma de Madrid under Projects CCG08 UC3M/MAT 4464 and CCG08 UC3M/DPI 4348.

References

[1] Tennyson RC. Composites in space – challenges and opportunities. Proc ICCM-10 1995;1:35–56.
[2] David-West OS, Nash DH, Banks WM. An experimental study of damage accumulation in balanced CFRP laminates due to repeated impact. Compos Struct 2008;83:247–58.
[3] Airoldi A, Cacchione B. Modelling of impact forces and pressures in Lagrangian bird strike analyses. Int J Impact Eng 2006;32:1651–77.
[4] Anghileri M, Castelleti LML, Invernizzi F, Mascheroni M. A survey of numerical models for hail impact analysis using explicit finite element codes. Int J Impact Eng 2005;31:929–44.
[5] Mines RAW, McKown S, Birch RS. Impact of aircraft rubber tyre fragments on aluminium alloy plates: I-experimental. Int J Impact Eng 2007;34:627–46.
[6] Varas D, López-Puente J, Zaera R. Experimental analysis of fluid-filled aluminium tubes subjected to high-velocity impact. Int J Impact Eng 2009;36:81–91.
[7] Varas D, Zaera R, López-Puente J. Numerical modelling of the hydrodynamic ram phenomenon. Int J Impact Eng 2009;36:363–74.
[8] Hai-jun X, Rong-ren W. Aeroengine turbine blade containment tests using high-speed rotor spin test facility. Aerospace Sci Technol 2006;10:501–8.
[9] Schonberg WP. Hole size and crack length models for spacecrafts walls under oblique hypervelocity projectile impact. Aerospace Sci Technol 1999;3:461–71.
[10] Farenthold EP, Hernandez RJ. Simulation of orbital debris impact on the space shuttle wing leading edge. Int J Impact Eng 2006;33:231–43.
[11] Cantwell WJ, Morton J. Comparison of low and high velocity impact response of CFRP. Composites 1989;20(6):545–51.
[12] Sun CT, Potti V. A simple model to predict residual velocities of thick composite laminates subjected to high velocity impact. Int J Impact Eng 1996;18(3):339–53.
[13] Larsson F. Damage tolerance of a stitched carbon/epoxy laminate. Composites Part A: Appl Sci Manufact 1997;28:923–34.
[14] Bland PW, Dear JP. Observations on the impact behaviour of carbon-fibre reinforced polymers for the qualitative validation of models. Composites Part A: Appl Sci Manufact 2001;32:1217–27.
[15] López-Puente J, Zaera R, Navarro C. The effect of low temperatures on the intermediate and high velocity impact response of CFRP. Composites: Part B 2002;33:559–66.
[16] López-Puente J, Zaera R, Navarro C. Experimental and numerical analysis of normal and oblique ballistic impacts on thin carbon/epoxy woven laminates. Composites: Part A 2008;39:374–87.
[17] Will MA, Franz T, Nurick GN. The effect of laminate stacking sequence of CFRP filament wound tubes subjected to projectile impact. Compos Struct 2002;58:259–70.
[18] Tanabe Y, Aoki M, Fujii K, Kasano H, Yasuda E. Fracture behavior of CFRPs impacted by relatively high-velocity steel sphere. Int J Impact Eng 2003;28:627–42.
[19] Tanabe Y, Aoki M. Stress and strain measurements in carbon-related materials impacted by a high-velocity steel sphere. Int J Impact Eng 2003;28:1045–59.
[20] Hammond RI, Proud WG, Goldrein HT, Field JE. High-resolution optical study of the impact of carbon-fibre reinforced polymers with different lay-ups. Int J Impact Eng 2004;30:69–86.
[21] Hosur MV, Vaidya UK, Ulven C, Jeelani S. Performance of stitched/unstitched woven carbon/epoxy composites under high velocity impact loading. Compos Struct 2004;64:455–66.
[22] Herzsberg I, Weller T. Impact damage resistance of buckled carbon/epoxy panels. Compos Struct 2006;73:130–7.
[23] Caprino G, Lopresto V, Santoro D. Ballistic impact behaviour of stitched graphite/epoxy laminates. Compos Sci Technol 2007;67:325–35.
[24] Hazell PJ, Kister G, Stennett C, Bourque P, Cooper G. Normal and oblique penetration of woven CFRP laminates by a high velocity steel sphere. Composites: Part A 2008;39:866–74.
[25] Kim H, Welch DA, Kedward KT. Experimental investigation of high velocity ice impacts on woven carbon/epoxy composite panels. Composites Part A: Appl Sci Manufact 2003;34:25–41.
[26] Chambers AR, Mowlem MC, Dokos L. Evaluating impact damage in CFRP using fibre optic sensors. Compos Sci Technol 2007;67:1235–42.
[27] Asp LE, Juntikka R. High velocity impact on NCF reinforced composites. Compos Sci Technol 2009;69(9):1478–82.
[28] Mines RAW, Roach AM, Jones N. High velocity perforation behaviour of polymer composite laminates. Int J Impact Eng 1999;22:561–88.
[29] Chen JK, Allahdadi FA, Carney TC. High-velocity impact of graphite/epoxy composite laminates. Compos Sci Technol 1997;57:1369–79.
[30] López-Puente J, Zaera R, Navarro C. High energy impact on woven laminates. J Phys IV 2003:639–44.
[31] Fernández-Fdz D, López-Puente J, Zaera R. Prediction of the behaviour of CFRPs against high-velocity impact of solids employing an artificial neural network methodology. Composites: Part A 2008;39:989–96.
[32] López-Puente J, Zaera R, Navarro C. An analytical model for high velocity impacts on thin CFRPs woven laminates. Int J Solids Struct 2007;44:2837–51.
[33] Schoeppner GA, Abrate S. Delamination threshold loads for low velocity impact on composite laminates. Composites: Part A 2000;431:903–15.
[34] Hazell PJ, Cowie A, Kister G, Stennett C, Cooper GA. Penetration of a woven CFRP laminate by a high velocity steel sphere impacting at velocities of up to 1875 m/s. Int J Impact Eng 2009;36(9):1136–42.